IEEE Access
Multidisciplinary | Rapid Review | Open Access Journal

Received August 10, 2017, accepted September 4, 2017, date of publication September 8, 2017,
date of current version September 27, 2017.

Digital Object Identifier 10.1109/ACCESS.2017.2750318

A Low Profile, Ultra-Lightweight, High Efficient Circularly-Polarized Antenna Array for Ku Band Satellite Applications

JIANQUAN HUANG[1], WEI LIN[2], (Member, IEEE), FENG QIU[1], CHUNZHI JIANG[1], DAJUN LEI[1], AND Y. JAY GUO[2], (Fellow, IEEE)

[1]School of Electronics Information and Electrical engineering, Xiangnan University, Chenzhou 423000, China
[2]Global Big Data Technologies Centre, University of Technology Sydney, Ultimo, NSW 2007, Australia

Corresponding author: Wei Lin (wei.lin@uts.edu.au)

This work was supported in part by the Natural Science Foundation of Hunan Province of China under Grant 2016JJ4083, in part by the Aid Program for Science and Technology Innovative Research Team in Higher Educational Institutions of Hunan Province, and in part by the Project Supported by Scientific Research Fund of Hunan Provincial Education Department under Grant 15CY009 and Grant 16A199, and in part by the Australian Research Council under Grant DP160102219.

ABSTRACT A novel low-profile, ultra-lightweight, high-efficient circularly polarized (CP) planar patch antenna array is reported for Ku-band satellite TV reception applications. The basic radiating element of the antenna array is realized by a 2×2 corner-removed patch subarray. This 2×2 patch subarray is center-fed by a rectangular coupling aperture etched on the top surface of a substrate-integrated-waveguide cavity. A novel compact sequential rotation feeding technique is adopted to broaden the operating bandwidth without occupying additional area. The 2×2 CP subarray can be easily scaled up for large size antenna arrays due to its single layer feeding network and compact radiating elements. In addition, the patch radiators are printed on a thin layer of Polyimide film backed by a piece of supporting foam to minimize the entire weight. To verify the design concept, a 96-element (16×6) CP patch array was fabricated and tested. Measured results show that the operating bandwidth is 700 MHz from 11.55 to 12.25 GHz. The gain is stable across the operating bandwidth with a realized peak gain of 26.4 dBic. The height of the antenna is 0.05 λ_0 and the total weight is only 66.5 g. It serves as an excellent candidate for Ku-band satellite applications.

INDEX TERMS CP antenna array, low profile, lightweight, Ku band satellite applications, SIW feeding network, sequentially rotating excitation method, patch antennas.

I. INTRODUCTION

Satellite communications undergoing rapid development recently, which provide many services such as navigation, weather forecasting, geo-imaging, data distribution, satellite phone and satellite TV broadcasting, etc. [1]–[4]. In particular, Ku band satellite TV applications are popular worldwide as they are robust for mobile platforms such as land vehicles, airplanes and ocean ships [5]–[7]. Traditional Ku band satellite antennas are commonly parabolic reflector antennas as shown in Fig. 1 which tend to be bulky and heavy. For instance, a commercial Ku band dish antenna from Fortec Star Inc. has a diameter of 65 cm and weight of 7 kg [8]. They are not desirable to be mounted on moving vehicles for satellite TV applications. Low profile and light weight planar antenna arrays are much preferred for such applications. In addition, circular polarization is more suited to satellite systems due to its polarization purity and the ability to avoid polarization mismatching [9]–[11].

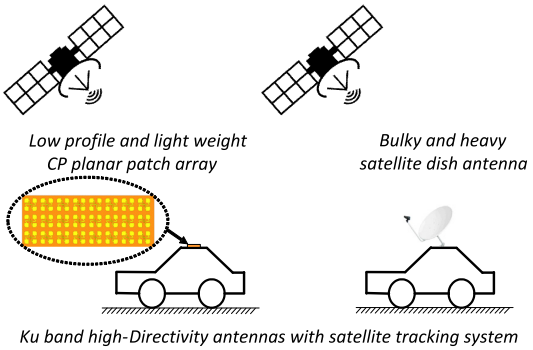

FIGURE 1. Illustration of Ku band high-directivity antennas with satellite tracking systems mounted on moving vehicles for satellite TV reception. (Left: The proposed low-profile and light weight CP planar array; Right: Traditional satellite dish antenna.)

To date, many efforts have been made on the designs of CP antenna arrays [12]–[25]. Various radiators such as helical antennas [12], spiral antennas [12], magneto-electric

dipoles [14], microstrip patches [15]–[21] and slot radiators [22]–[25] can all be employed as the basic radiating element to construct a CP antenna array. Existing feeding networks for CP arrays are mainly based on microstirp lines, striplines and waveguides including coplanar waveguides and substrate-integrated-waveguides (SIW). The profile and overall weight of the CP antenna array are dependent on both the types of the radiating elements and the feeding network structures. For example, 4×4 helical radiators with a stripline feeding network were realized by LTCC technology in [12]. Due to the 3D structure of the helical radiator, the profile of this CP array is about 0.36 λ_0 (λ_0 refers to the wavelength of the lowest operating frequency) and the fabrication cost is potentially high. Another design in [13] adopts two-arm spiral radiators as the basic radiating element that is fed by two layers of SIW networks. As the original bi-directional radiating spiral radiator needs to be placed above a reflector with approximately a quarter wavelength distance to achieve broadside radiation, the total profile of this design is 0.45 λ_0. Similarly in [14], an 8 × 8 ME dipole CP antenna array was fed by two layers of SIW networks. The profile is 0.44 λ_0. To realize a low profile CP array, planar microstrip patch radiators are good candidates due to their low profile nature. For instance, 2 × 2 cavity-backed modified circular patch radiators fed by SIW network is proposed in [14]. The profile achieved is 0.18 λ_0 with three PCB substrates. In addition, the design in [16] adopted 4 × 4 aperture-fed corner-removed square patch radiators with a microstrip line feeding network. The overall profile was further reduced to 0.16 λ_0. But the structure is complicated that requires assembling four pieces of PCB substrates. In addition to patch radiators, slot radiators etched on the surface of cavities like the SIW cavities are also good candidates for realizing low profile CP arrays. Specifically, the design in [22] realized an 8 × 8 SIW cavity-backed slot CP array. The profile of this design is 0.12 λ_0 with two PCB substrates. All above designs discussed and those in [17]–[21] require at least two pieces of PCB substrates. In order to further reduce the profile, and the weight and loss introduced by the substrate, CP antenna array constructed by a single PCB substrate is preferred. One antenna design in [25] utilized the series SIW feeding network with 4 × 4 slot radiators etched on the top of a SIW cavity. Although it has a single PCB substrate with a low profile of 0.03 λ_0, the operating bandwidth is only 1% and the configuration is not particularly suited for larger scale arrays.

In this paper, we propose a compact, low profile (0.05 λ_0), ultra-lightweight (66.5 gram), high-efficient (65%), 96 elements (16 × 6) CP antenna array constructed with a PCB substrate, a piece of supporting foam and a layer of Polyimide film with metallic patterns. To realize these superior characteristics, we designed a novel and compact SQR feeding structure to excite the microstrip subarray patches. Compared with the traditional 1 to 4 SQR feeding network that requires longer arms and larger area, the proposed SQR network has a natural out-of-phase SIW to microstrip transition which minimizes the overall area of the feeding structure. In addition, the patch radiators are printed on a thin layer of Polyimide film backed by a piece of supporting foam to minimize the entire weight. The obtained operating bandwidth of the CP antenna array is 700 MHz from 11.55 to 12.25 GHz. The realized peak gain is 26.4 dBic.

The paper is organized as follows. Following this Introduction, Section II presents the initial design of the aperture-coupled 2 × 2 CP patch subarray. To increase the operating bandwidth of the original design, the sequentially rotating (SQR) feeding technique is introduced to the 2×2 CP patch subarray in Section III. The operating bandwidth is increased by more than three times than the initial design. Finally, the design of a 96 elements (16 × 6) array and the experimental results are discussed in Section IV. Section V presents the conclusions.

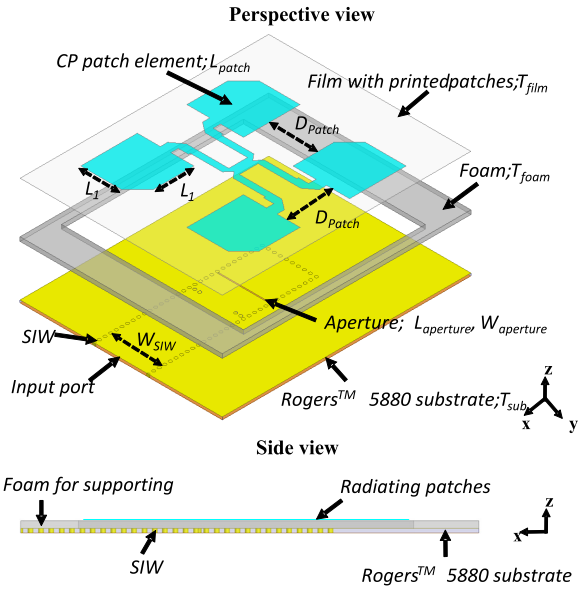

FIGURE 2. Configuration of the original 2 × 2 CP subarray. (Top): Perspective view by different layers; and (Bottom): Side view of the low profile subarray entity.

II. INITIAL DESIGN OF APERTURE-COUPLED 2 × 2 CP PATCH SUBARRAY

The initial designed aperture-coupled CP 2 × 2 subarray is shown in Fig. 2, which consists of three parts from top to bottom. The 2 × 2 radiating patches are etched on a piece of Polyimide film that is on the top layer. The thickness of the Polyimide film is 0.1 mm and the dielectric constant is about 3. The four radiating patches are formed from a square patch by removing different corners and fed by microstrip lines from the side. All the four radiators are circularly polarized. The side length of the square patch is L_{patch} and the length of the corner-removed side is L_1. Below the Polyimide film is a piece of supporting foam with the thickness of 0.8 mm. The regions of the foam beneath the radiating patches are removed for two purposes. First, the total weight of a large scale array can be further reduced. Second, dielectric losses are minimized. The bottom part of

TABLE 1. Original CP subarray parameters.

Parameter	Description	Value
L_{patch}	Length of the square radiating patches	11.2 mm
L_1	Length of the patch at the notched side	8.1 mm
D_{patch}	Distance between the patches	9.8 mm
$L_{subarray}$	Total side length of the CP subarray	40 mm
$L_{aperture}$	Length of the aperture	10 mm
L_{cavity}	Length of the SIW cavity	14.24 mm
$W_{opening}$	Width of opening of the SIW cavity	6.5 mm
$W_{aperture}$	Width of the aperture	0.22 mm
W_{SIW}	Width of the SIW	10.7 mm
T_{film}	Thickness of patch Polyimide film	0.1 mm
T_{foam}	Thickness of foam	0.8 mm
T_{sub}	Thickness of the substrate	0.508 mm

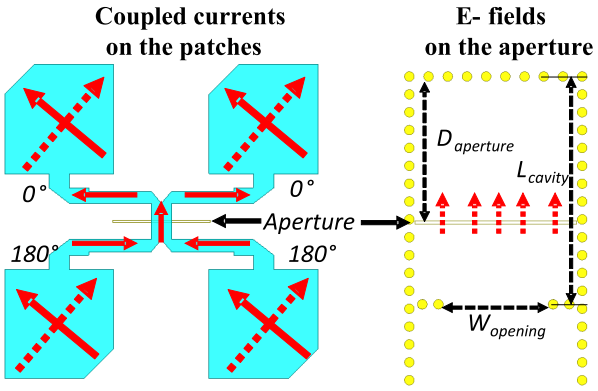

FIGURE 3. Top view of the coupled current directions and phases on the radiating patches of the 2 × 2 CP subarray.

this CP array is the coupling aperture feeding based on a SIW with width of W_{SIW}. The SIW is fabricated on a block of Rogers^{TM} 5880 copper-cladded substrate with the thickness of 0.508 mm. Its relative permittivity and permeability are 2.2 and 1.0 respectively; its loss tangent is 0.0009. As shown in Fig. 3, four short vias are arranged inside the SIW to construct a cavity with the length of L_{cavity} and the opening of $W_{openning}$. A rectangular aperture with the length of $L_{Aperture}$ and width of $W_{Aperture}$ is created on the top surface of the SIW cavity. The total thickness of this subarray is only 1.408 mm ($0.05\lambda_0$), where λ_0 refers to the lowest operating frequency of the antenna. The detailed parameters are listed in Table 1.

The aperture coupling feeding technique in this 2 × 2 CP subarray design is the key to realizing the compact radiating array structure. This feeding technique was previously introduced in [26] but that antenna array was linearly-polarized. In this design, we adopt the corner-removed radiating patch to obtain the CP radiation for satellite applications. As seen in Fig. 3, the rectangular aperture provides the differential excitations for the patches. As a result, the current distributions on the four patches are in the same direction at any given time. If the corners are removed at the diagonal position between the upper and below patches, a 2 × 2 CP antenna array is constructed.

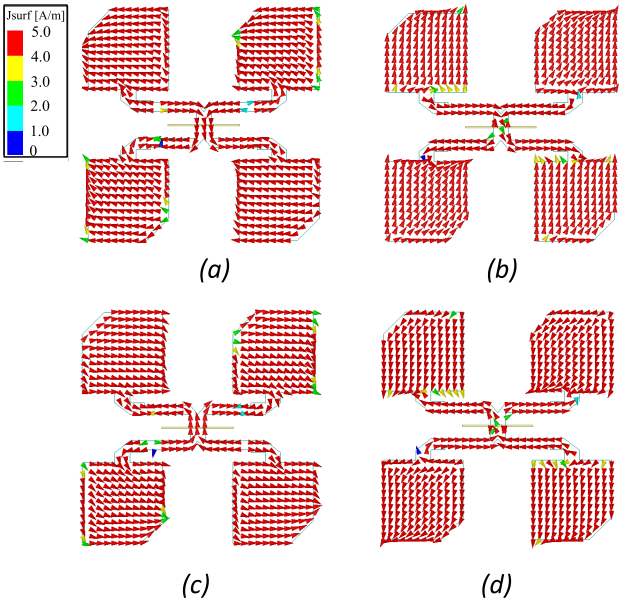

FIGURE 4. Current distribution on the patches of the CP subarray in a period of time at 12 GHz. (a) $t = 0$. (b) $t = 1/4\ T$. (c) $t = 2/4\ T$. (d) $t = 3/4\ T$.

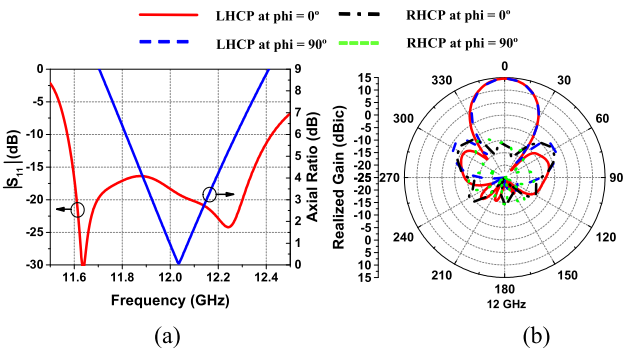

FIGURE 5. Simulated results of the original aperture-coupled CP subarray. a) $|S_{11}|$ and axial ratio values as functions of the source frequency, and (b) Realized gain patterns at 12 GHz.

Figure 4 shows the currents distributions on the CP subarray in a period of time. It is clearly seen that the currents on all the four patches are rotating simultaneously in the clockwise manner. Consequently, the LHCP broadside radiation is realized as the current movement follows the left-handed rule.

Simulated $|S_{11}|$, axial ratio values and radiation patterns are presented in Fig. 5. It is observed that the 3-dB AR bandwidth falls into the −10-dB impedance bandwidth. The overlapped AR and impedance bandwidth is 220 MHz from 11.92 to 12.14 GHz. Good uni-directional CP radiation patterns at the two vertical planes are also realized with a peak realized gain of 14.4 dBic. However, the achieved operating bandwidth of this CP subarray design is only 1.8%. Owing to the demand of larger channel capacity, CP antenna arrays with larger bandwidth are desired for satellite communications. Based on this initial subarray, a modified design is further developed with a novel and compact sequential rotation (SQR) feeding technique that largely increases the

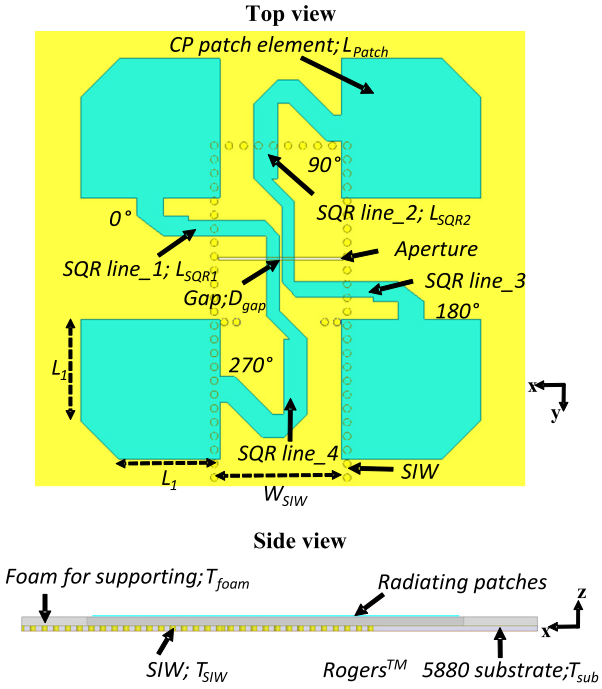

FIGURE 6. Configuration of the 2 × 2 CP subarray with the sequential rotation (SQR) excitations. (Top): Top view of the antenna; and (Bottom): Side view of the low profile subarray.

operating bandwidth by more than three times. In the following Sections, we will first discuss the modified 2 × 2 CP subarray with SQR feeding as the basic radiating element and then present the expanded array design and measured results of the final 6 × 16 large scale CP array.

III. APERTURE-FED 2 × 2 CP PATCH ARRAY WITH COMPACT SEQUENTIAL ROTATION (SQR) EXCITATIONS

A. ANTENNA CONFIGURATION AND PERFORMANCE

It is well known that circular polarization is realized by the two degenerated modes on the corner-removed patch antenna. As seen in Fig, 6, the solid and dashed arrows represent the two desegregated modes (marked as "a" and "b") on the patch. The essential 90° phase difference between the two modes is determined by the offset between the resonant frequencies of the two modes. This phase difference is very sensitive to the operating frequency of the antenna. As a result, the AR bandwidth is narrow. This method to realize CP radiation is also called "self-phase shifting" method as used in previous CP patches [27], helical antennas [4] and CP orthogonal dipoles [28].

To increase the AR bandwidth of CP antennas, one method is to adopt the sequential rotation (SQR) excitations as in [29]–[31]. The fundamental reason for the AR bandwidth enhancement by SQR excitation technique is the stable amplitude and phase difference among the four excitations within a wide frequency range.

In this paper, we successfully applied the SQR feeding concept to largely increase the AR bandwidth by more than three times than the initial design. The novel antenna

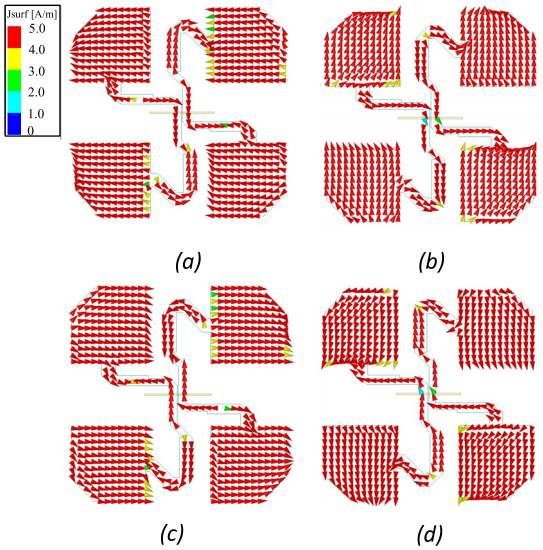

FIGURE 7. Current distributions on the patches of the CP subarray with SQR excitations in a period of time at 12 GHz. (a) $t = 0$. (b) $t = 1/4\ T$. (c) $t = 2/4\ T$. (d) $t = 3/4\ T$.

configuration of the 2 × 2 CP subarray with the SQR excitations is shown in Fig. 6. The whole antenna structure is similar to the initial design except for the top microstrip feeding lines and the orientation of the patches. This SQR feeding structure is much more compact compared with the traditional 1 to 4 SQR microstrip feeding network that requires longer arms because a natural out-of-phase SIW to microstrip transition is employed in this design. Unlike the united feeding line of the original design, the feeding line of the modified design is split into two parts in the center. In addition, the feeding lines for Patch#2 and Patch#4 are quarter wavelength longer than the feeding lines of Patch#1 and Patch#3. Consequently, the phases of the excitations for the four patches (Patch#1 to Patch#4) are 0°, 90°, 180° and 270°, respectively. It is noted that the removed corners of the four patches are also sequentially rotated. In this manner, both the two degenerated modes will rotate clockwise to generate the CP radiation. As the amplitude and phase of the SQR feeding are stable enough to cover a wide frequency spectrum, wider AR bandwidth is realized. Figure 7 presents the current distributions on the patches in a period of time at 12GHz. It is observed that the currents on each patch are rotating clockwise so that the LHCP broadside radiation is generated.

Figure 8 exhibits the simulated performance of the CP subarray with SQR feeding. The overlapped 3-dB AR and −10 dB impedance bandwidth is 780 MHz from 11.77 to 12.55 GHz, which is more than three times wider than the operating bandwidth 220MHz of the initial design. The realized gain is very stable across the entire operating bandwidth with the peak value of 14.9 dBic. Good radiation patterns at two vertical planes ($\varphi = 0°$ and $\varphi = 90°$) at 12 GHz are also obtained with the side lobe lower than −15 dB. Wide AR beamwidth of 53° is achieved. The above simulated results clearly demonstrated that wide operating bandwidth is realized by the SQR feeding techniques.

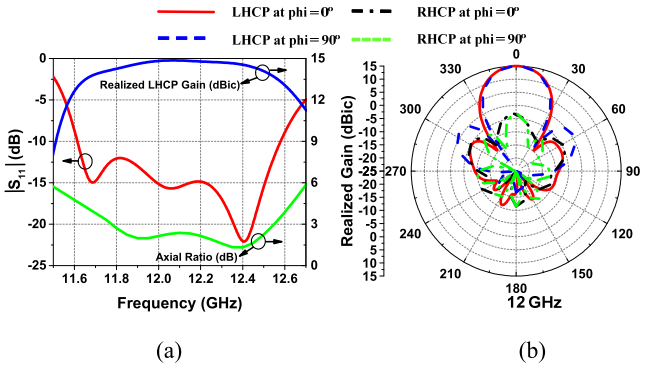

FIGURE 8. Simulated results of the aperture-coupled CP subarray with SQR feeding. a) $|S_{11}|$, axial ratio values and realized gain as functions of the source frequency, and (b) Realized gain patterns at 12 GHz.

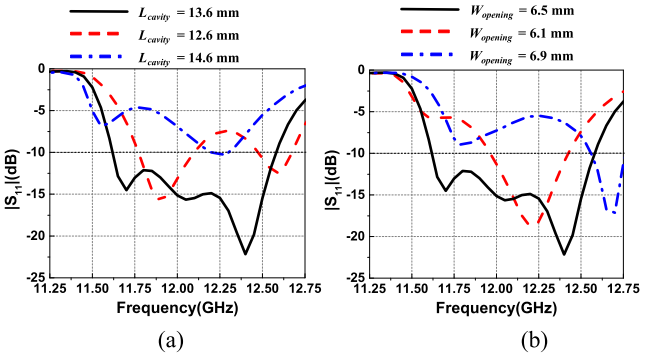

FIGURE 9. Study of the resonant cavity beneath the radiating patch. a) $|S_{11}|$ as functions of the source frequency when the length of the cavity is 12.6 mm, 13.6 mm and 14.6 mm, and (b) $|S_{11}|$ as functions of the source frequency when the width of the cavity opening is 6.1 mm, 6.5 mm and 6.9 mm.

TABLE 2. SQR CP subarray parameters.

Parameter	Description	Value
L_1	Length of the patch at the notched side	7.8 mm
D_{gap}	Gap between the two center SQR lines	0.22 mm
W_{SQR1}	Width of narrow SQR feeding line	1 mm
W_{SQR2}	Width of wider SQR feeding line	2.1 mm
L_{SQR1}	Length of shorter SQR line	14.6 mm
L_{SQR2}	Length of longer SQR line	21.4 mm

The entire structure is compact and low profile, which is very suitable to be used as the basic radiating element for constructing large scale antenna arrays. The unique antenna parameters in this design are listed in Table 2 and all other parameters are as same as the original design in Table 1.

B. KEY PARAMETRICS STUDY AND DESIGN GUIDELINE

In this part, we will discuss three critical design considerations in this 2 × 2 CP subarray with SQR feeding technique, such as the dimension of the SIW resonating cavity beneath the patch radiators; the position and length of the coupling aperture; the size and profile of the radiation patches. The above analysis provides the guideline for the general design of similar antennas at different frequencies.

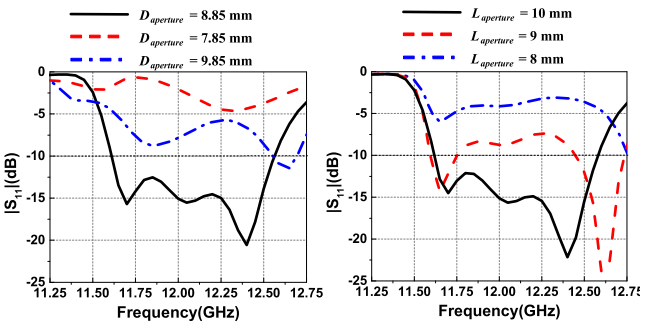

FIGURE 10. Study of the coupling aperture. a) $|S_{11}|$ as functions of the source frequency when the aperture position $D_{aperture}$ is 7.85 mm, 8.85 mm and 9.85 mm, and (b) $|S_{11}|$ as functions of the source frequency when the length of the aperture is 8 mm, 9 mm and 10 mm.

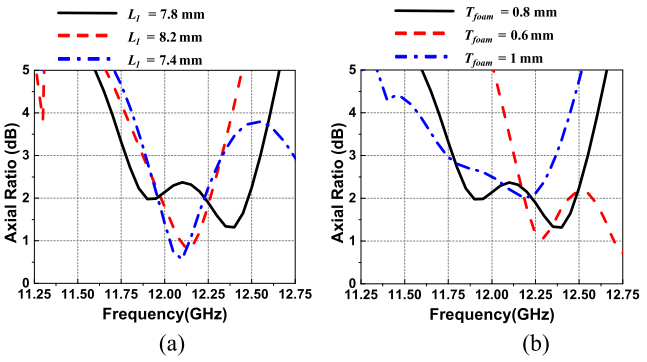

FIGURE 11. Study of the radiating patch. a) Axial Ratio as functions of the source frequency when the patch length of L_1 is 7.4 mm, 7.8 mm and 8.2 mm, and (b) Axial Ratio as functions of the source frequency when the profile of the patch above ground plane is 0.6 mm, 0.8 mm and 1 mm.

1) SIW RESONATING CAVITY

The dimension of the SIW resonating cavity determines the resonant frequency and is sensitive to the impedance matching of the proposed CP subarray. As seen in Fig. 3, four shorting vias inside the SIW form a cavity beneath the four patches with the length of L_{cavity} and opening width of $W_{opening}$. The resonant mode is TE_{110} mode in the SIW cavity. Fig. 9 shows the $|S_{11}|$ values as functions of the source frequency when L_{cavity} and $W_{opening}$ are varying. It is observed that the two parameters are very sensitive to the impedance matching. As in Fig. 9 (a), when the cavity length changes from 12.6 to 14.6 mm with the interval of 1mm, the resonances move toward the lower band and the impedance matching changes greatly. In addition, Fig. 9 (b) exhibits that the cavity opening width $W_{opening}$ varying from 6.1 to 6.9 mm with the interval of 1 mm is also critical to the impedance matching. Finally, the optimized values $L_{cavity} = 13.6$ mm ($0.54\lambda_c$) and $W_{opening} = 6.5$ mm ($0.26\lambda_c$) are selected. (λ_c refers to the center operating frequency.)

2) COUPLING RECTANGULAR APERTURE

Another important parameter is the coupling rectangular aperture that will determine the coupling level from the

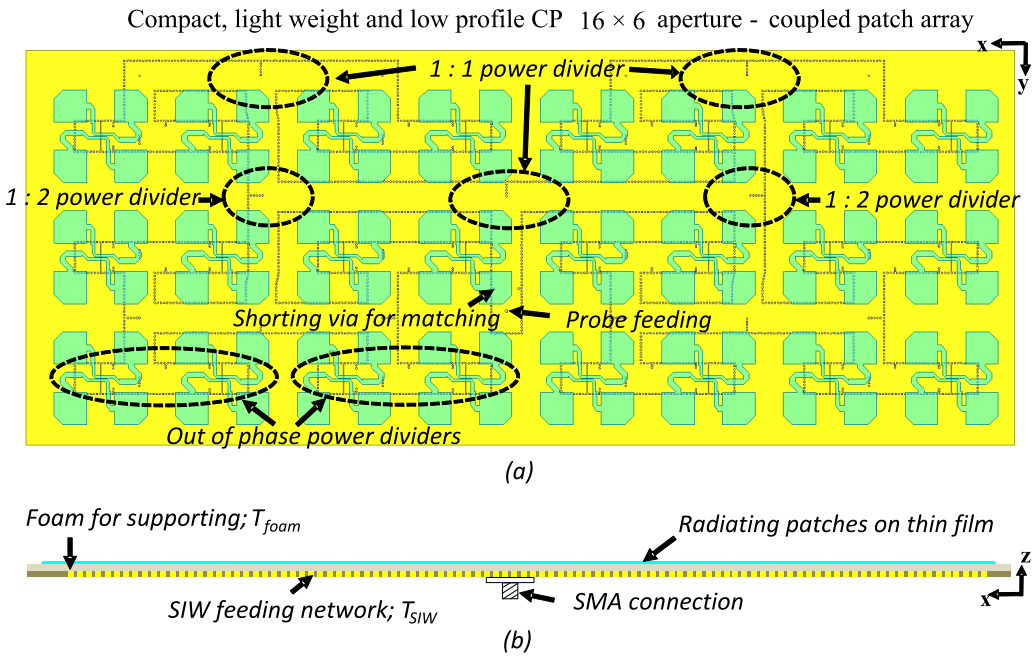

FIGURE 12. Configuration of the compact, light weight and low profile 16 × 6 CP patch array with SIW feeding network. (a): Top view; and (b): Side view.

SIW cavity to the patch radiators. Both the position $D_{aperture}$ and the length $L_{aperture}$ of the aperture will affect the coupling level as well as the impedance matching. Fig. 10 presents the returns loss values as $D_{aperture}$ and $L_{aperture}$ are varying. It is seen that both parameters are sensitive to the impedance matching. The optimized values $D_{aperture} = 8.85$ mm $(0.35\lambda_c)$ and $L_{aperture} = 10$ mm $(0.4\lambda_c)$ are chosen for the final design. Moreover, it is noted that the width of the aperture should be design as 1/50 of the length of the aperture.

3) RADIATING PATCHES

The dimension and profile of the radiating patches will determine the axial ratio bandwidth of the CP subarray. It is well-known that the operating frequency of a square patch radiator is determined by the length L_{patch} and the CP performance is dependent on the length L_1 on the side with the notch. In the final prototype, L_{patch} is design as 0.45 λ_c. In addition, the profile T_{foam} of the patches also affects the AR bandwidth. Fig. 11 presents the AR values as functions of the source frequency when L_{patch} and T_{foam} are varying. Both the parameters are sensitive to the AR bandwidth. The optimized value $L_1 = 7.8$ mm $(0.7L_{patch})$ and $T_{foam} = 0.8$ mm are selected for the final design.

4) DESIGN GUIDELINE

The design guideline for arbitrary frequency operation is concluded as below:

The first step is to design the SIW feeding structure, which was thoroughly analyzed in [32] and [33]. The width of the SIW W_{SIW} is set to $0.4\lambda_c$ in the initial design if the dielectric constant of the substrate is 2.2 as the Rogers^{TM} 5880.

The second step is to determine the dimension of the cavity with the coupling aperture. The length of the SIW cavity L_{cavity} and the opening width $W_{opening}$ can be set to $0.54\lambda_c$ and $0.26\ \lambda_c$, respectively in the initial design. Later, a rectangular aperture is etched on the top surface of the SIW with the distance $L_{aperture} = 0.35\ \lambda_c$ towards the end. The length of the aperture $L_{aperture}$ is set to the same as the width of the SIW W_{SIW}.

The third step is to design the SQR feeding line and the associated radiating patches. To match the impedance of the coupling aperture, the characteristic impedance of the microstrip line section above the aperture is set to 110 ohm (width is 1 mm). The microstrip line section to feed the patch is set to 75 ohm (width is 2.1 mm), which matches the radiation impedance of the corner-notched patch. To provide the 90° phase difference, the SQR line_2 is quarter wavelength longer than the SQR line_1 as seen in Fig. 6. SQR line_3 is identical to SQR line_1 and SQR line_4 is identical to SQR line_2. Finally, the initial size of the patch L_{patch} and L_1 are set to 0.45 λ_c and $0.7L_{patch}$, respectively.

IV. IMPLEMENTATION AND MEASURED RESULTS OF THE 96-ELEMENT (16 × 6) CP PATCH ARRAY

Based on above CP subarray design, we successfully expanded it into a 96-element 16 × 6 array as shown in Fig. 12. 24 CP subarrays are arranged into three rows, which are fed by a 1 to 24 SIW feeding network. To provide the balanced excitation for each subarray, both 1:1 and 1:2 SIW power dividers are adopted. In addition, to provide the correct phase for the neighboring subarrays, out-of-phase SIW power dividers are also used. The entire SIW feeding

TABLE 3. Design comparisons of the cp antenna arrays reported in the literature to date.

Ref.	Radiating elements	Realized Gain (dBic)	Peak Radiation efficiency	Components for assembly	Profile (λ_0)	Cost	Fabrication Complexity
[16]	4 × 4	15	N. A.	Multi-layer LTCC	0.39	High	Complex
[11]	4 × 4	14	53%	Multi-layer LTCC	0.36	High	Complex
[17]	4 × 4	16	N. A.	Multi-layer LTCC	0.2	High	Complex
[15]	4 × 4	17.1	N. A.	Multi-layer LTCC	0.16	High	Complex
[22]	4 × 4	18.7	N. A.	3 PCBs + 1 Metal base	0.39	Moderate	Moderate
[12]	4 × 4	19.5	87.1%	3 PCBs	0.45	Moderate	Moderate
[13]	8 × 8	26.1	72.2	3 PCBs	0.44	Moderate	Moderate
[18]	4 × 4	18.2	65	3 PCBs	0.18	Moderate	Moderate
[19]	4 × 4	15.8	N. A.	4 PCBs	0.14	Moderate	Moderate
[14]	2 × 2	12.5	N. A.	3 PCBs	0.18	Moderate	Moderate
[21]	16 × 16	25.9	N. A.	2 PCBs	0.12	Moderate	Moderate
Our design	16 × 6	**26.4**	**65%**	**1 PCB + 1 Foam + 1 Film (66.5 gram)**	**0.05**	**Low**	**Simple**

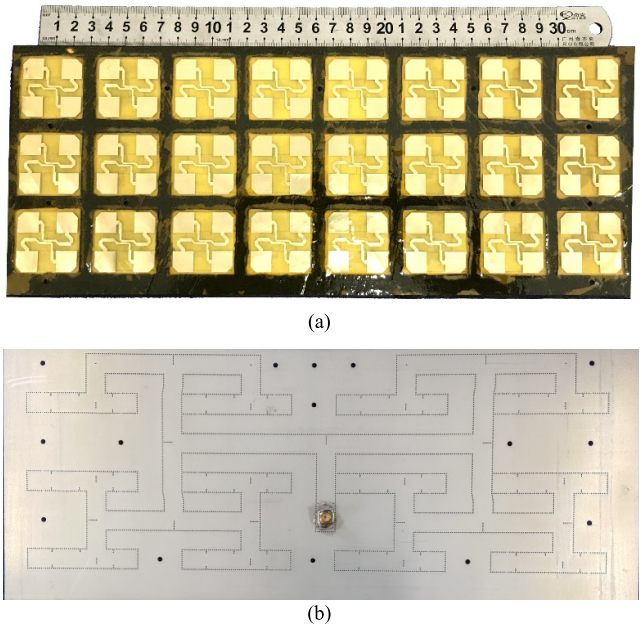

FIGURE 13. Fabricated antenna array model. a) Top view, and (b) Bottom view.

structure is very compact. The array components were fabricated and assembled as in Fig. 13. The radiating patches were etched on a piece of Polyimide film. The 1 to 24 SIW feeding network is fabricated on a block of Rogers^{TM} 5880 copper-cladded substrate by standard PCB manufacturing technology. A piece of sticky supporting foam was placed between the film and the SIW substrate to provide the correct gap between the patches and the SIW surface. The rectangular areas of the foam beneath the patches were removed for further decreasing the total weight and loss of the array. The final prototype achieved very low profile of $0.05\lambda_0$ and the total weight is only 66.5 gram. The overall size of the array is 340 mm ($13\lambda_0$) × 137 mm ($5.3\lambda_0$). The $|S_{11}|$ of the antenna

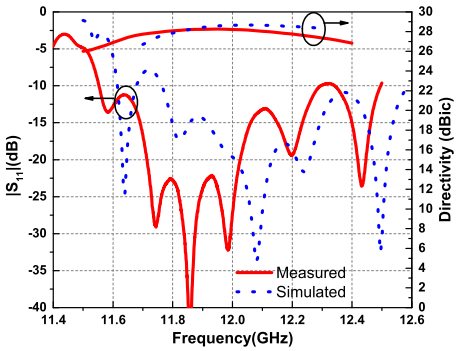

FIGURE 14. Measured and simulated $|S_{11}|$ and directivity of fabricated antenna array.

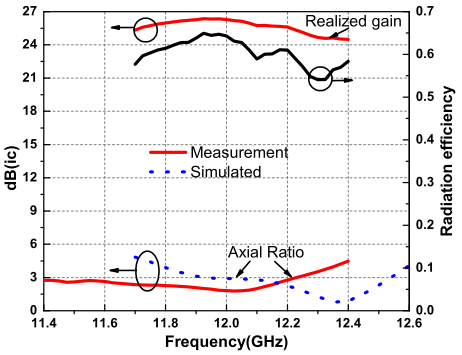

FIGURE 15. Measured and simulated Axial Ratio, gain and radiation efficiency.

was measured with a Keysight N5230C vector network analyzer and the radiation pattern was measured by the Near-field antenna measurement system. All the simulated results were obtained with the Ansoft HFSS EM solver version 17.

Measured and simulated $|S_{11}|$ and directivity are shown in Fig. 14, which are in reasonable agreement. The measured −10 dB impedance bandwidth is 750 MHz from 11.55 to 12.3 GHz. It slightly shifts to the lower band than the

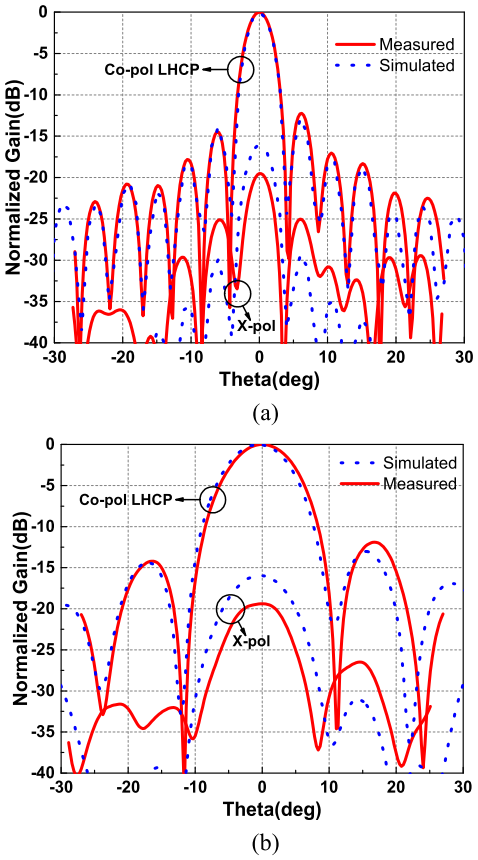

FIGURE 16. **Measured and simulated radiation patterns at 12 GHz. (a) $\varphi = 0°$ plane. (b) $\varphi = 90°$ plane.**

simulation. Measured directivity is stable across the impedance bandwidth with the peak value of 28.6 dBic.

Figure 15 presents the measured and simulated AR bandwidth, gain and radiation efficiency. In consistent with the impedance bandwidth, the AR bandwidth slightly shifts to the lower band that covers 850MHz from 11.4 to 12.25 GHz. Consequently, the overlapped impedance & AR bandwidth is 700 MHz from 11.55 to 12.25 GHz. The measured realized gain is stable cross the entire operating bandwidth with the peak value of 26.4 dBic. The peak measured radiation efficiency is 65% which is decent for such large scale array. The losses are mainly due to the insertion loss of the 1 to 24 SIW power divider and the copper loss of the radiating patches. The simulated and measured radiation patterns at 12 GHz are compared in Fig. 16, both agree with each other very well.

The above measured results exhibit the excellent radiation performance of the proposed CP antenna array. Importantly, it is very low profile (0.05 λ_0), ultra-lightweight (66.5 gram), high efficient (65%) and low-cost & simple fabrication. Table 3 compares various characteristics between the reported CP antenna arrays and our design. It is concluded that our design achieves the lowest profile and very light weight. The fabrication process is simple and low-cost. The realized gain and efficiency are decent. It is an ideal candidate for *ku* band mobile satellite applications.

V. CONCLUSION

A low-profile, ultra-lightweight and high efficient CP antenna array is presented in the paper. Two designs of aperture-fed 2 × 2 patch subarrays were presented at the beginning. Based on the initial subarray with out of phase excitations, we designed a novel and compact sequential rotation (SQR) feeding technique to broaden the operating bandwidth for more than three times than the original design. Based on the subarray as the basic radiating element, we expanded it into a 96-element 16 × 6 patch array. Measured results show excellent CP radiation performance with decent bandwidth, realized gain and radiation pattern. Meanwhile, it is very low-profile, ultra-lightweight and high efficient. It is a good candidate for wireless systems preferring high gain CP antennas, in particular, *Ku* band satellite communication applications.

REFERENCES

[1] S.-I. Jeon, Y.-W. Kim, and D.-G. Oh, "A new active phased array antenna for mobile direct broadcasting satellite reception," *IEEE Trans. Broadcast.*, vol. 46, no. 1, pp. 34–40, Mar. 2000.

[2] A. R. Weily and Y. J. Guo, "Circularly polarized ellipse-loaded circular slot array for millimeter-wave WPAN applications," *IEEE Trans. Antennas Propag.*, vol. 57, no. 10, pp. 2862–2870, Oct. 2009.

[3] W. Lin and H. Wong, "Circularly polarized conical-beam antenna with wide bandwidth and low profile," *IEEE Trans. Antennas Propag.*, vol. 62, no. 12, pp. 5974–5982, Dec. 2014.

[4] Q.-X. Chu, W. Lin, W.-X. Lin, and Z.-K. Pan, "Assembled dual-band broadband quadrifilar helix antennas with compact power divider networks for CNSS application," *IEEE Trans. Antennas Propag.*, vol. 61, no. 2, pp. 516–523, Feb. 2013.

[5] M. T. Zhang *et al.*, "Design of novel reconfigurable reflectarrays with single-bit phase resolution for Ku-band satellite antenna applications," *IEEE Trans. Antennas Propag.*, vol. 64, no. 5, pp. 1634–1641, May 2016.

[6] S. Ye *et al.*, "High-gain planar antenna arrays for mobile satellite communications [antenna applications corner]," *IEEE Antennas Propag. Mag.*, vol. 54, no. 6, pp. 256–268, Dec. 2012.

[7] J. Huang *et al.*, "A new compact and high gain circularly-polarized slot antenna array for Ku-band mobile satellite TV reception," *IEEE Access*, vol. 5, pp. 6707–6714, May 2017.

[8] "Data sheet of the 65 cm Ku band offset dish antenna," Fortec Star Inc., Appl. Note. [Online]. Available: http://www.viasatelital.com

[9] H. Wong, W. Lin, L. Huitema, and E. Arnaud, "Multi-polarization reconfigurable antenna for wireless biomedical system," *IEEE Trans. Biomed. Circuits Syst.*, vol. 11, no. 3, pp. 652–660, Jun. 2017.

[10] W. Lin and H. Wong, "Wideband circular-polarization reconfigurable antenna with L-shaped feeding probes," *IEEE Antenna Wireless Propag. Lett.*, vol. 16, pp. 2114–2117, Apr. 2017, doi: 10.1109/LAWP.2017.2699289.

[11] W. Lin and H. Wong, "Multipolarization-reconfigurable circular patch antenna with L-shaped probes," *IEEE Antenna Wireless Propag. Lett.*, vol. 16, pp. 1549–1552, 2017.

[12] C. Liu, Y.-X. Guo, X. Bao, and S.-Q. Xiao, "60-GHz LTCC integrated circularly polarized helical antenna array," *IEEE Trans. Antennas Propag.*, vol. 60, no. 3, pp. 1329–1335, Mar. 2012.

[13] Q. Zhu, K.-B. Ng, and C. H. Chan, "Printed circularly polarized spiral antenna array for millimeter-wave applications," *IEEE Trans. Antennas Propag.*, vol. 65, no. 2, pp. 636–643, Feb. 2017.

[14] Y. Li and K.-M. Luk, "A 60-GHz wideband circularly polarized aperture-coupled magneto-electric dipole antenna array," *IEEE Trans. Antennas Propag.*, vol. 64, no. 4, pp. 1325–1333, Apr. 2016.

[15] A. B. Guntupalli and K. Wu, "60-GHz circularly polarized antenna array made in low-cost fabrication process," *IEEE Antennas Wireless Propag. Lett.*, vol. 13, pp. 864–867, 2014.

[16] W. Zhang, Y. P. Zhang, M. Sun, C. Luxey, D. Titz, and F. Ferrero, "A 60-GHz circularly-polarized array antenna-in-package in LTCC technology," *IEEE Trans. Antennas Propag.*, vol. 61, no. 12, pp. 6228–6232, Dec. 2013.

[17] Y. Li, Z. N. Chen, X. Qing, Z. Zhang, J. Xu, and Z. Feng, "Axial ratio bandwidth enhancement of 60-GHz substrate integrated waveguide-fed circularly polarized LTCC antenna array," *IEEE Trans. Antennas Propag.*, vol. 60, no. 10, pp. 4619–4626, Oct. 2012.
[18] H. Sun, Y.-X. Guo, and Z. Wang, "60-GHz circularly polarized U-slot patch antenna array on LTCC," *IEEE Trans. Antennas Propag.*, vol. 61, no. 1, pp. 430–435, Jan. 2013.
[19] J. Wu, Y. J. Cheng, and Y. Fan, "Millimeter-wave wideband high-efficiency circularly polarized planar array antenna," *IEEE Trans. Antennas Propag.*, vol. 64, no. 2, pp. 535–542, Feb. 2016.
[20] H. W. Lai, D. Xue, H. Wong, K. K. So, and X. Y. Zhang, "Broadband circularly polarized patch antenna arrays with multiple-layers structure," *IEEE Antennas Wireless Propag. Lett.*, vol. 16, pp. 525–528, 2017.
[21] M. Li and K.-M. Luk, "Low-cost wideband microstrip antenna array for 60-GHz applications," *IEEE Trans. Antennas Propag.*, vol. 62, no. 6, pp. 3012–3018, Jun. 2014.
[22] D.-F. Guan, C. Ding, Z.-P. Qian, Y.-S. Zhang, Y. J. Guo, and K. Gong, "Broadband high-gain SIW cavity-backed circular-polarized array antenna," *IEEE Trans. Antennas Propag.*, vol. 64, no. 4, pp. 1493–1497, Apr. 2016.
[23] Y. Lang, S.-W. Qu, and J.-X. Chen, "Wideband circularly polarized substrate integrated cavity-backed antenna array," *IEEE Antennas Wireless Propag. Lett.*, vol. 13, pp. 1513–1516, 2014.
[24] J. M. F. González, P. Padilla, G. Expósito-Domínguez, and M. Sierra-Castañer, "Lightweight portable planar slot array antenna for satellite communications in X-band," *IEEE Antennas Wireless Propag. Lett.*, vol. 10, pp. 1409–1412, 2011.
[25] Z. C. Hao, X. Liu, X. Huo, and K. K. Fan, "Planar high-gain circularly polarized element antenna for array applications," *IEEE Trans. Antennas Propag.*, vol. 63, no. 5, pp. 1937–1948, May 2015.
[26] Y. J. Cheng, Y. X. Guo, and Z. G. Liu, "W-band large-scale high-gain planar integrated antenna array," *IEEE Trans. Antennas Propag.*, vol. 62, no. 6, pp. 3370–3373, Jun. 2014.
[27] H. Wong, K.-M. Luk, C. H. Chan, Q. Xue, K. K. So, and H. W. Lai, "Small antennas in wireless communications," *Proc. IEEE*, vol. 100, no. 7, pp. 2109–2121, Jul. 2012.
[28] A. Nešić, V. Branković, and I. Radnović, "Circularly polarised printed antenna with conical beam," *Electron. Lett.*, vol. 34, no. 12, pp. 1165–1167, Jun. 1998.
[29] B. Lee and Y. Yoon, "Low-profile, low-cost, broadband millimeter-wave antenna array for high-data-rate WPAN systems," *IEEE Antennas Wireless Propag. Lett.*, vol. 16, pp. 1957–1960, Apr. 2017, doi: 10.1109/LAWP.2017.2690440.
[30] W. Lin and H. Wong, "Wideband circular polarization reconfigurable antenna," *IEEE Trans. Antennas Propag.*, vol. 63, no. 12, pp. 5938–5944, Dec. 2015.
[31] Q. Wu, H. Wang, C. Yu, and W. Hong, "Low-profile circularly polarized cavity-backed antennas using SIW techniques," *IEEE Trans. Antennas Propag.*, vol. 64, no. 7, pp. 2832–2839, Jul. 2016.
[32] L. Yan, W. Hong, G. Hua, J. Chen, K. Wu, and T. J. Cui, "Simulation and experiment on SIW slot array antennas," *IEEE Microw. Wireless Compon. Lett.*, vol. 14, no. 9, pp. 446–448, Sep. 2004.
[33] D. Deslandes and K. Wu, "Accurate modeling, wave mechanisms, and design considerations of a substrate integrated waveguide," *IEEE Trans. Microw. Theory Techn.*, vol. 54, no. 6, pp. 2516–2526, Jun. 2006.

JIANQUAN HUANG received the M.S. degree from Hunan Normal University, Changsha, Hunan, and the Ph.D. degree from the South China University of Technology, Guangzhou, China. Since 2012, he has been an Associate Professor with Xiangnan University, Chenzhou, China, where he is also currently charging the Microwave Communication Joint Laboratory. He is also charging Gospell. He is currently visiting the Global Big Data Technologies Centre, University of Technology Sydney, Australia.

His research interests are mainly in the fields of circularly polarized planar antenna and array and reconfigurable planar antenna.

WEI LIN (M'16) received the bachelor's and master's degrees in electronic engineering from the South China University of Technology, Guangzhou, China, in 2009 and 2012, respectively, and the Ph.D. degree in electronic engineering from the City University of Hong Kong, Hong Kong, in 2016. He was a Research Associate with Nanyang Technological University, Singapore, from 2012 to 2013.

He is currently a Post-Doctoral Research Fellow with the Global Big Data Technologies Centre, University of Technology Sydney, Sydney, Australia. He received the Outstanding Master Thesis Award from the South China University of Technology in 2013, the Young Scientist Award at the IEEE Region 10 Conference in 2015, and the Talent Development Scholarship from the Hong Kong SAR Government in 2016. His research interests include designs of reconfigurable antennas, HF antennas, satellite antennas, millimeter wave antennas, and terahertz devices and applications.

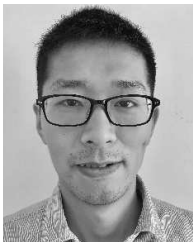

FENG QIU received the B.S and M.S degrees in electrical and information engineering from Xidian University, Xi'an, in 2012 and 2015, respectively. Since 2015, he has been a Lecturer with Xiangnan University, Chenzhou, China. His research interests are predominantly in the field of microwave components using dielectric resonators and circularly polarized planar antennas and antenna arrays.

CHUNZHI JIANG received the M.S. degree from the National University of Defense Technology, Changsha, China. She has been a Professor with the School of Electronic Information and Electrical Engineering, Xiangnan University, Chenzhou, since 2014. Her research interests are mainly in the fields of electromagnetic field theory and applications.

DAJUN LEI received the B.S. degree from Hunan Normal University in 1996 and the Ph.D. degree from Hunan University, Changsha, China, in 2011.

He is currently a Professor with the School of Electronic Information and Electrical Engineering, Xiangnan University, Chenzhou. His research interests are mainly in the fields of dielectric resonator microwave components and planar antennas and arrays.

Y. JAY GUO (F'14) received the bachelor's and master's degrees from Xidian University, China, in 1982 and 1984, respectively, and the Ph.D. degree from Xian Jiaotong University, China, in 1987. He has authored over 300 research papers, and he holds 22 patents in antennas and wireless systems. His research interest includes antennas, mm-wave and THz communications, sensing systems, as well as big data. He is a fellow of the Australian Academy of Engineering and Technology and the IET, and a member of the College of Experts of Australian Research Council. He has received a number of most prestigious Australian national awards, and was named one of the most influential engineers in Australia in 2014 and 2015.

In 2014, he served as a Director of CSIRO for over nine years, directing a number of ICT research portfolios. Before joining CSIRO, he held various senior leadership positions at Fujitsu, U.K., Siemens, U.K., and NEC, U.K. He is currently a Distinguished Professor and the founding Director of the Global Big Data Technologies Centre, University of Technology Sydney, Australia.

Prof Guo has chaired numerous international conferences. He was the International Advisory Committee Chair of the IEEE VTC2017, the General Chair of ISAP2015, iWAT2014, and WPMC'2014, and the TPC Chair of 2010 IEEE WCNC, and 2012 and 2007 IEEE ISCIT. He served as the Guest Editor of special issues on Antennas for Satellite Communications and Antennas and Propagation Aspects of 60–90 GHz Wireless Communications, both in the IEEE TRANSACTIONS ON ANTENNAS AND PROPAGATION, special issue on Communications Challenges and Dynamics for Unmanned Autonomous Vehicles, the IEEE JOURNAL ON SELECTED AREAS IN COMMUNICATIONS, and Special Issue on 5G for Mission Critical Machine Communications, the *IEEE Network Magazine*.